

# The One Component Plasma as a red thread for two dimensional Physics

Riccardo Fantoni\*

*Università di Trieste, Dipartimento di Fisica, strada Costiera 11, 34151 Grignano (Trieste), Italy*  
(Dated: December 30, 2025)

We review the Two-Dimensional One-Component Plasma, i.e. the non-quantum electron gas on a surface. We allow for a curvature of the surface and discuss some exact analytical solutions at a special value of the coupling constant. Then we recall how this system has a central role in the construction of the Laughlin trial wave function for the fractional quantum Hall effect. We then recall how the same system is also central for the universal jump in the superfluid fraction of a fluid of bosons at the critical temperature for the superfluid transition. We conclude with some remarks on a numerical simulation of the superfluid fraction in a quantum many body superfluid on a curved surface with path integral.

Keywords: Surface; One-Component Plasma; Laughlin Wave Function; Superfluid Fraction; Universality

## CONTENTS

I. Introduction	2
II. On a curved surface	2
A. The surface	2
B. The Coulomb potential	3
C. The background	3
D. The total potential energy	3
E. The densities and distribution functions	4
III. On the plane	4
A. The Coulomb potential	4
B. The background	5
C. The total potential energy	5
D. Partition function and densities at a special temperature	5
IV. Discussion for the 2D OCP on various curved surfaces	6
V. The Laughlin trial wave function	7
A. The Landau problem	7
B. The Laughlin problem	8
VI. The Nelson-Kosterlitz phase transition	9
A. Renormalization method	11
VII. Calculation of the superfluid fraction with path integral	11
A. Algorithm description	12
B. The superfluid fraction	13
Area estimator	14
Winding estimator	15
In $d = 2$	15
VIII. Concluding remarks	15
A. The high temperature density matrix on Riemannian manifolds	16
On a sphere	17

---

\* riccardo.fantoni@scuola.istruzione.it

Author declarations	18
Conflicts of interest	18
Data availability	18
Funding	18
References	18

## I. INTRODUCTION

A *One Component Plasma* (OCP) is a system of  $N$  pointwise identical non-quantum particles of charge  $e$  embedded in a uniform neutralizing background of opposite charge [1]. In the quantum regime this is usually called *Jellium*. It is the simplest many body model for an electron gas.

We will review the two dimensional OCP in flat and curved spaces [2], Laughlin trial wave function for the fractional quantum Hall effect [3], and Kosterlitz phase transition in a two dimensional superfluid [4, 5]. All these two dimensional problems have the OCP at the heart of their solution. From this point of view it is interesting to see how the OCP acted as a red thread for very different aspects of two dimensional physics.

## II. ON A CURVED SURFACE

### A. The surface

We will generally consider *Riemannian surfaces*  $\mathcal{S}$  with a coordinate frame  $\mathbf{q} = (x^1, x^2)$  and with a metric

$$ds^2 = g_{\mu\nu}(\mathbf{q}) dx^\mu dx^\nu, \quad (2.1)$$

with  $g_{\mu\nu}$  the metric tensor and a sum over repeated indexes is tacitly assumed. We will denote with  $g(\mathbf{q})$  the Jacobian of the transformation to an orthonormal coordinate reference frame, i.e. the determinant of the metric tensor  $g_{\mu\nu}$ . The surface may be embeddable in the three dimensional space or not. It is important to introduce a *disk*  $\Omega_R$  of radius  $R$  and its boundary  $\partial\Omega_R$ . The connection coefficients, the Christoffel symbols, in a coordinate frame are

$$\Gamma_{\mu\beta\gamma} = \frac{1}{2}(g_{\mu\beta,\gamma} + g_{\mu\gamma,\beta} - g_{\beta\gamma,\mu}), \quad (2.2)$$

where the comma denotes a partial derivative as usual. The Riemann tensor in a coordinate frame reads

$$R^\alpha{}_{\beta\gamma\delta} = \Gamma^\alpha{}_{\beta\delta,\gamma} - \Gamma^\alpha{}_{\beta\gamma,\delta} + \Gamma^\alpha{}_{\mu\gamma}\Gamma^\mu{}_{\beta\delta} - \Gamma^\alpha{}_{\mu\delta}\Gamma^\mu{}_{\beta\gamma}, \quad (2.3)$$

in a two-dimensional space has only  $2^2(2^2 - 1)/12 = 1$  independent component. The scalar curvature is then given by the following indexes contractions (the trace of the Ricci curvature tensor),

$$R = R^\mu{}_\mu = R^{\mu\nu}{}_{\mu\nu}, \quad (2.4)$$

and the (intrinsic) Gaussian curvature is  $K = R/2$ . In an embeddable surface we may define also a (extrinsic) mean curvature  $H = (k_1 + k_2)/2$ , where the principal curvatures  $k_i$ ,  $i = 1, 2$  are the eigenvalues of the shape operator or equivalently the second fundamental form of the surface and  $1/k_i$  are the principal radii of curvature. The Euler characteristic of the disk  $\Omega_R$  is given by

$$\chi = \frac{1}{2\pi} \left( \int_{\Omega_R} K dS + \int_{\partial\Omega_R} k dl \right), \quad (2.5)$$

where  $dS = \sqrt{g(\mathbf{q})} d\mathbf{q}$  is the elementary surface area on  $\mathcal{S}$  and  $k$  is the geodesic curvature of the boundary  $\partial\Omega_R$ .

The Weyl conformal tensor is defined as follows [6]

$$C^{\alpha\beta}{}_{\gamma\delta} = R^{\alpha\beta}{}_{\gamma\delta} - 2\delta_{[\gamma}{}^{[\alpha} R_{\delta]}{}^{\beta]} + \frac{1}{3}\delta_{[\gamma}{}^{[\alpha}\delta_{\delta]}{}^{\beta]} R, \quad (2.6)$$

where indexes in square brackets are antisymmetrized.

The Weyl conformal tensor has the following properties:

- i. Has same symmetries of Riemann;

- ii. Is completely trace-free, i.e. contraction of  $C_{\alpha\beta\gamma\delta}$  on any two indexes vanishes. It can be considered as the trace-free part of Riemann.
- iii. In a manifold  $\mathcal{M}$  of dimension  $d$ , its number of independent components can be inferred by the two properties above. Recalling the counting for Riemann and noticing that property [ii.] above requires that contracting any two indexes we are left with only other two indexes with the proper symmetry constraints we conclude that the number of independent components of the Weyl tensor is given by  $d^2(d^2 - 1)/12 - d(d + 1)/2$  for  $d \geq 3$  so it must be 0 for  $d \leq 3$ . Thus for  $d \leq 3$  we may assume that the Weyl tensor is identically zero and the Riemann tensor is completely determined by its trace, the Ricci tensor,
- iv.  $C^{\alpha\beta}_{\gamma\delta} = 0$  if and only if  $\mathcal{M}$  is *conformally flat*, i.e. if and only if it is reducible to a flat space by a *conformal transformation*, i.e. if and only if it exists a coordinate frame where

$$ds^2 = e^{2\phi(x^\alpha)} \eta_{\alpha\beta} dx^\alpha dx^\beta, \quad (2.7)$$

with  $\phi$  a scalar. The function  $e^\phi$  is called the *conformal factor*.

## B. The Coulomb potential

The *Coulomb potential*  $G(\mathbf{q}, \mathbf{q}_0)$  created at  $\mathbf{q}$  by a unit charge at  $\mathbf{q}_0$  is given by the Green function of the Laplacian

$$\Delta G(\mathbf{q}, \mathbf{q}_0) = -2\pi\delta^{(2)}(\mathbf{q}; \mathbf{q}_0), \quad (2.8)$$

with appropriate boundary conditions. Here  $\Delta = \partial_\alpha(\sqrt{g}g^{\alpha\beta}\partial_\beta)/\sqrt{g}$ , with  $\partial_\alpha = \partial/\partial x^\alpha$ , is the Laplace-Beltrami operator. This equation can often be solved by using the decomposition of  $G$  as a Fourier series.

## C. The background

The Coulomb potential generated by the *background*, with a constant surface charge density  $\rho_b = -en_b$  satisfies the Poisson equation

$$\Delta v_b = -2\pi\rho_b. \quad (2.9)$$

The Coulomb potential of the background can be obtained by solving Poisson equation with the appropriate boundary conditions. Also, it can be obtained from the Green function computed in the previous section

$$v_b(\mathbf{q}) = \int G(\mathbf{q}, \mathbf{q}') \rho_b(\mathbf{q}') dS'. \quad (2.10)$$

This integral can be performed easily by using the Fourier series decomposition of Green's function  $G$ .

## D. The total potential energy

The *total potential energy* of the plasma is then

$$\begin{aligned} V_N &= V_N^{pp} + V_N^{pb} + V_N^0 = \frac{e^2}{2} \sum_{i \neq j} G(|\mathbf{q}_i - \mathbf{q}_j|) + e \sum_i \int_{\Omega_R} v_b(|\mathbf{q} - \mathbf{q}_i|) dS + \\ &\quad \frac{1}{2} \iint_{\Omega_R} \rho_b v_b(|\mathbf{q} - \mathbf{q}'|) dS dS', \end{aligned} \quad (2.11)$$

where the last term  $V_N^0$  is the self energy of the background and the first two terms  $V_N^{pp}$  and  $V_N^{pb}$  are the interaction potential energy between the charges at  $\mathbf{q}_i$ ,  $i = 1, \dots, N$  and between the charges and the background, respectively.

### E. The densities and distribution functions

Given either the canonical partition function in a fixed region  $\Omega \in \mathcal{S}$  of a Riemannian surface  $\mathcal{S}$ ,  $Z_N(\Gamma)$  with  $\Gamma = \beta e^2$  the coupling constant, or the grand canonical one  $\Xi[\{\lambda_p(\mathbf{q})\}, \Gamma]$ , with  $\lambda_p$  some position dependent fugacities, we can define the *n-body density functions*. Denoting with  $\mathbf{p} = (p, \mathbf{q})$  the species  $p$  and the position  $\mathbf{q}$  of a particle of this species, we have,

$$\begin{aligned} & \rho^{(n)}(\mathbf{p}_1, \dots, \mathbf{p}_n; N, \Gamma) \\ &= \rho(\mathbf{p}_1; N, \Gamma) \cdots \rho(\mathbf{p}_n; N, \Gamma) g_{p_1 \dots p_n}(\mathbf{q}_1, \dots, \mathbf{q}_n; N, \Gamma) \\ &= \left\langle \sum_{i_1, \dots, i_n} {}^{DP} \delta^{(2)}(\mathbf{q}_1; \mathbf{q}_{i_1}) \delta_{p_1, p_{i_1}} \cdots \delta^{(2)}(\mathbf{q}_n; \mathbf{q}_{i_n}) \delta_{p_n, p_{i_n}} \right\rangle_{N, \Gamma}, \end{aligned} \quad (2.12)$$

where  $\delta_{p,q}$  is the Kronecker delta,  $\delta^{(2)}$  is the Dirac delta function on the curved surface such that  $\int \delta^{(2)}(\mathbf{q}; \mathbf{q}') dS = 1$  with  $dS = \sqrt{g(\mathbf{q})} d\mathbf{q}$  the elementary surface area on  $\mathcal{S}$ ,  $\langle \dots \rangle_{N, \Gamma} = \sum_{p_1, \dots, p_N} \int_{\Omega} \dots e^{-\beta V_N} dS_1 \cdots dS_N / Z_N$  is the thermal average in the canonical ensemble,  $\sum^{DP}$  denotes the inclusion in the sum only of addends containing the product of delta functions relative to different particles, and we omitted the superscript <sup>(1)</sup> in the one-body densities. The  $g_{p_1, \dots, p_n}$  are known as the *n-body distribution functions*. It is convenient to introduce another set of correlation functions which decay to zero as two groups of particles are largely separated [7], namely the *truncated* (Ursell) correlation functions,

$$\rho^{(n)T}(\mathbf{p}_1, \dots, \mathbf{p}_n; N, \Gamma) = \rho^{(n)}(\mathbf{p}_1, \dots, \mathbf{p}_n; N, \Gamma) - \sum \prod_{m < n} \rho^{(m)T}(\mathbf{p}_{i_1}, \dots, \mathbf{p}_{i_m}; N, \Gamma), \quad (2.13)$$

where the sum of products is carried out over all possible partitions of the set  $(1, \dots, n)$  into subsets of cardinal number  $m < n$ .

In terms of the grand canonical partition function we will have,

$$\rho^{(n)}(\mathbf{p}_1, \dots, \mathbf{p}_n; \{\lambda_p\}, \Gamma) = \prod_{i=1}^n \lambda_{p_i}(\mathbf{q}_i) \frac{1}{\Xi[\{\lambda_p\}, \Gamma]} \frac{\delta^{(n)} \Xi[\{\lambda_p\}, \Gamma]}{\delta \lambda_{p_1}(\mathbf{q}_1) \dots \delta \lambda_{p_n}(\mathbf{q}_n)}, \quad (2.14)$$

and

$$\rho^{(n)T}(\mathbf{p}_1, \dots, \mathbf{p}_n; \{\lambda_p\}, \Gamma) = \prod_{i=1}^n \lambda_{p_i}(\mathbf{q}_i) \frac{\delta^{(n)} \ln \Xi[\{\lambda_p\}, \Gamma]}{\delta \lambda_{p_1}(\mathbf{q}_1) \dots \delta \lambda_{p_n}(\mathbf{q}_n)}. \quad (2.15)$$

We may also use the notation  $\rho^{(n)}(\mathbf{p}_1, \dots, \mathbf{p}_n; \{\lambda_p\}, \Gamma) = \rho_{p_1 \dots p_n}^{(n)}(\mathbf{q}_1, \dots, \mathbf{q}_n; \{\lambda_p\}, \Gamma)$  where for example in the two-component mixture each  $p = \pm$  denotes either a positive or a negative charge. And sometimes we may omit the dependence from the number of particles, the fugacities, and the coupling constant. From the structure it is possible to derive the thermodynamic properties of the plasma (but not the contrary).

### III. ON THE PLANE

The metric tensor in the Cartesian coordinates  $\mathbf{q} = (x, y)$  of the plane is,

$$\|g_{\mu\nu}\| = \begin{pmatrix} 1 & 0 \\ 0 & 1 \end{pmatrix}, \quad (3.1)$$

with  $g = 1$  and the curvature is clearly zero. We will use polar coordinates  $\mathbf{q} = (r, \varphi)$  with  $r = \sqrt{x^2 + y^2}$  and  $\varphi = \arctan(y/x)$ .

#### A. The Coulomb potential

The Coulomb interaction potential between a particle at  $\mathbf{q}$  and a particle at  $\mathbf{q}_0$  a distance  $r = |\mathbf{q} - \mathbf{q}_0|$  from one another is

$$G(\mathbf{q}, \mathbf{q}_0) = -\ln(|\mathbf{q} - \mathbf{q}_0|/L), \quad (3.2)$$

where  $L$  is a length scale.

## B. The background

If one assumes the particles to be confined in a disk  $\Omega_R = \{\mathbf{q} \in \mathcal{S} | 0 \leq \varphi \leq 2\pi, 0 \leq r \leq R\}$  of area  $\mathcal{A}_R = \pi R^2$  the background potential is

$$v_b(r) = en_b \frac{\pi}{2} \left( r^2 - R^2 + 2R^2 \ln \frac{R}{L} \right), \quad (3.3)$$

where  $r = |\mathbf{q}|$ .

## C. The total potential energy

The total potential energy of the system is then given by Eq. (2.11). Developing all the terms and using  $n_b = n = N/\mathcal{A}_R$  (this is not a necessary condition since we can imagine a situation where  $n_b \neq n$ . In this case the system would not be electrically neutral) we then find

$$V_N/e^2 = - \sum_{i < j} \ln \left( \frac{r_{ij}}{L} \right) + \frac{n_b \pi}{2} \sum_i r_i^2 + n_b^2 \pi^2 R^4 \left( -\frac{3}{8} + \frac{1}{2} \ln \frac{R}{L} \right), \quad (3.4)$$

where  $r_{ij} = |\mathbf{q}_i - \mathbf{q}_j|$  and  $r_i = |\mathbf{q}_i|$ . This can be rewritten as follows

$$V_N/e^2 = - \sum_{i < j} \ln \left( \frac{r_{ij}}{R} \right) + \frac{N}{2} \sum_i \left( \frac{r_i}{R} \right)^2 + \quad (3.5)$$

$$N^2 \left( -\frac{3}{8} + \frac{1}{2} \ln \frac{R}{L} \right) - \frac{N(N-1)}{2} \ln \left( \frac{R}{L} \right). \quad (3.6)$$

We can then introduce the new variables [8]  $\mathbf{z}_i = \sqrt{N} \mathbf{q}_i / R$  to find

$$V_N/e^2 = f(\{\mathbf{z}_i\}) + f_c \quad (3.7)$$

$$f = - \sum_{i < j} \ln z_{ij} + \frac{1}{2} \sum_i z_i^2, \quad (3.8)$$

$$f_c = \frac{N(N-1)}{4} \ln(n\pi L^2) + N^2 \left( -\frac{3}{8} + \frac{1}{2} \ln \frac{R}{L} \right). \quad (3.9)$$

We can always choose  $L = R$  so that in the thermodynamic limit  $\lim_{N \rightarrow \infty} f_c/N = -\ln(n\pi L^2)/4$  and the excess Helmholtz free energy per particle

$$a_{\text{exc}} = F_{\text{exc}}/N \rightarrow -\frac{e^2}{4} \ln(\pi n L^2) + a_0(T), \quad (3.10)$$

with  $a_0$  some function of the temperature  $T$  alone. Therefore, the equation of state has the simple form

$$p = (1/\beta - e^2/4)n, \quad (3.11)$$

where  $\beta = 1/k_B T$  with  $k_B$  Boltzmann's constant.

## D. Partition function and densities at a special temperature

At the special temperature  $T_0 = e^2/2k_B$  the partition function can be found exactly analytically using the properties of the van der Monde determinant [8, 9]. Using polar coordinates  $\mathbf{z}_i = (z_i, \theta_i)$ , one obtains at  $T_0$  a Boltzmann factor

$$e^{-\beta V_N} = A_N e^{-\sum_i z_i^2} \left| \prod_{i < j} (Z_i - Z_j) \right|^2, \quad (3.12)$$

where  $A_N$  is a constant and  $Z_i = z_i \exp(i\theta_i)$ . This expression can be integrated upon variables  $\mathbf{z}_i$  ( $0 \leq z_i \leq \sqrt{N}$ ) by expanding the van der Monde determinant  $\prod(Z_i - Z_j)$ . One obtains the partition function

$$Z_N(2) = \int e^{-\beta V_N} d\mathbf{z}_1 \cdots d\mathbf{z}_N = A_N \pi^N N! \prod_{j=1}^N \gamma(j, N), \quad (3.13)$$

where

$$\gamma(j, N) = \int_0^{\sqrt{N}} e^{-z^2} z^{2(j-1)} 2z dz = \int_0^N e^{-t} t^{j-1} dt, \quad (3.14)$$

is the incomplete gamma function. Taking the thermodynamic limit of  $-\ln(Z_N(2)/\mathcal{A}_R^N)]/N \rightarrow \beta a_{\text{exc}}(2)$  we obtain the Helmholtz free energy per particle

$$a_{\text{exc}}(2) = -\frac{e^2}{4} \ln(\pi n L^2) + \frac{e^2}{2} \left[ 1 - \frac{1}{2} \ln(2\pi) \right]. \quad (3.15)$$

One can also obtain the  $n$ -body distribution functions from the truncated densities [7] as follows

$$g(1, \dots, n; N) = e^{-\sum_{i=1}^n z_i^2} \det [K_N(Z_i \bar{Z}_j)]_{i,j=1,\dots,n}, \quad (3.16)$$

where  $\bar{Z}$  is the complex conjugate of  $Z$  and

$$K_N(x) = \sum_{i=1}^N \frac{x^{i-1}}{\gamma(i, N)}. \quad (3.17)$$

In the thermodynamic limit  $N \rightarrow \infty$ ,  $\gamma(i, N) \rightarrow (i-1)!$ , and  $K_N(x) \rightarrow e^x$ . In this limit, one obtains from Eq. (3.16) the following explicit distribution functions [8]

$$g(1) = 1, \quad (3.18)$$

$$g(1, 2) = 1 - e^{-\pi n r_{12}^2}, \quad (3.19)$$

$$g(1, 2, 3) = \dots \quad (3.20)$$

This Gaussian falloff is in agreement with the general result according to which, among all possible long-range pair potentials, it is only in the Coulomb case that a decay of correlations faster than any inverse power is compatible with the structure of equilibrium equations like the Born-Green-Yvon hierarchic set (see Ref. [7] section II.B.3). A somewhat surprising result is that the correlations does not have the typical exponential falloff typical of the high-temperature Debye-Hückel approximation [10]. One easily checks that the distribution functions obey the perfect screening and other sum rules.

Expansions around  $\Gamma = 2$  suggests that the pair correlation function changes from the exponential form to an oscillating one for a region with  $\Gamma > 2$ . This behavior of the pair correlation function as the coupling is stronger has been observed in Monte Carlo simulations [11]. For sufficient high values of  $\Gamma$  (low temperatures) the 2D OCP begins to crystallize and there are several works where the freezing transition is found. For the case of the sphere Caillol et al. [11] localized the coupling parameter for melting at  $\Gamma \approx 140$ . In the limit  $\Gamma \rightarrow \infty$  the 2D OCP becomes a Wigner crystal. In particular, the spatial configuration of the charges which minimizes the energy at zero temperature for the 2D OCP on a plane is the usual hexagonal lattice. The Wigner crystal of the 2D OCP on sphere or the Thomson problem has been studied numerically in Ref. [12].

#### IV. DISCUSSION FOR THE 2D OCP ON VARIOUS CURVED SURFACES

The OCP is exactly solvable at any temperatures in one dimension [13, 14]. In two dimensions [2], Jancovici and Alastuey [8, 9, 15, 16] proved that the OCP is exactly solvable analytically at a special value of the coupling constant,  $\Gamma = \beta e^2 = 2$  where  $\beta = 1/k_B T$  with  $k_B$  Boltzmann's constant and  $T$  the absolute temperature, on a plane. Since then, a growing interest in two-dimensional plasmas has lead to study this system on various flat geometries [17–19] and two-dimensional curved surfaces like the cylinder [20, 21], the sphere [22–25], the pseudosphere [26–28], and Flamm paraboloid [29] (see Fig. 1). Among these surfaces only the last one, due to Flamm, is of non-constant curvature. The sphere is the surface of constant positive curvature and the pseudosphere is the surface of constant negative curvature.

These studies are certainly relevant for the properties of graphene [30] even if we do not expect extraordinary new phenomenon due to the effect of the surface curvature on the electronic properties of these new materials [31].

Much more compelling and of fundamental importance is the bridge that these studies build between the two scientific communities of the exact simulations of a many body (quantum) system and of general relativity. We foresee an important progress in the physics of (quantum) gravity of many body systems beyond simple ideal gases or hydrodynamic systems [32].

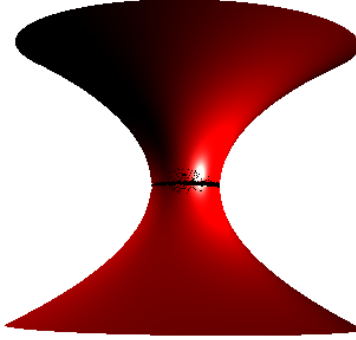


FIG. 1. A Flamm paraboloid. A surface of non-constant curvature.

## V. THE LAUGHLIN TRIAL WAVE FUNCTION

In this section we study the properties of many electrons on a plane immersed in a constant uniform magnetic field orthogonal to the plane.

### A. The Landau problem

An electron moving [33] in an electric field  $\mathbf{E} = -\nabla\varphi$  and a magnetic field  $\mathbf{B} = \nabla \times \mathbf{A}$ , where  $\mathbf{A}$  is the vector potential, is subject to the Lorentz force which in Gaussian units reads  $\mathbf{F} = q(\mathbf{E} + \frac{\mathbf{v}}{c} \times \mathbf{B})$  where  $q = -e$  is the electron charge,  $\mathbf{v}$  is the speed of the electron, and  $c$  is the speed of light. In order to reach to this result from the Hamilton equations of motion it is necessary to start with a classical Hamiltonian  $H = \frac{1}{2m}(\mathbf{p} - \frac{q}{c}\mathbf{A})^2 + q\varphi$ . This amounts to the following transformation recipe  $\mathbf{p} \rightarrow \mathbf{p} - \frac{q}{c}\mathbf{A}$ . If we start from a quantum Hamiltonian  $H = \frac{1}{2m}\mathbf{p}^2 = \frac{1}{2m}(\boldsymbol{\sigma} \cdot \mathbf{p})(\boldsymbol{\sigma} \cdot \mathbf{p})$ , where  $\boldsymbol{\sigma} = (\sigma_1, \sigma_2, \sigma_3)$  and  $\sigma_i$  are the Pauli matrices such that  $(\boldsymbol{\sigma} \cdot \mathbf{A})(\boldsymbol{\sigma} \cdot \mathbf{B}) = \mathbf{A} \cdot \mathbf{B} + i\boldsymbol{\sigma} \cdot (\mathbf{A} \times \mathbf{B})$  for any two operators  $\mathbf{A}$  and  $\mathbf{B}$ . After applying the transformation recipe required by classical electrodynamics we find

$$H = \frac{1}{2m} \left( \mathbf{p} - \frac{q}{c} \mathbf{A} \right)^2 - \frac{q\hbar}{2mc} \boldsymbol{\sigma} \cdot \mathbf{B} + q\varphi, \quad (5.1)$$

where we have used  $\mathbf{p} \times \mathbf{A} = -i\hbar(\nabla \times \mathbf{A}) - \mathbf{A} \times \mathbf{p}$ . A gauge transformation  $\mathbf{A} \rightarrow \mathbf{A} + \nabla f$ ,  $\varphi \rightarrow \varphi - (\partial f / \partial t)/c$  must leave the Schrödinger equation unchanged which can be accomplished upon changing  $\psi \rightarrow \psi e^{iqf/\hbar c}$  so that  $|\psi|^2$  does not change.

Consider an two dimensional electron gas in the  $(x, y)$  plane subjected to a magnetic field  $\mathbf{B}$  in the  $z$  direction. Landau [34] chooses a gauge with  $A_x = -By$ ,  $A_y = A_z = 0$  so that  $\mathbf{B} = \hat{z}B$ ,  $\nabla \mathbf{A} = 0$ ,  $[p_x, H] = [p_z, H] = 0$ , and we may choose

$$\psi = e^{i(p_x x + p_z z)/\hbar} \chi(y). \quad (5.2)$$

Schrödinger equation then becomes

$$\chi'' + \frac{2m}{\hbar^2} \left[ \left( E + \frac{q\hbar\sigma_z}{2mc} B - \frac{p_z^2}{2m} \right) - \frac{1}{2} m\omega_B^2 (y - y_0)^2 \right] \chi = 0, \quad (5.3)$$

where  $y_0 = -cp_x/qB$  and  $\omega_B = |q|B/mc$ . We then recognize the harmonic oscillator equation in the  $y$  direction with solution

$$E_n = \left( n + \frac{1}{2} \right) \hbar\omega_B - \frac{q\hbar\sigma_z}{2mc} B + \frac{p_z^2}{2m}, \quad (5.4)$$

$$\chi_n(y) = \frac{1}{\pi^{1/4} a_B^{1/2} \sqrt{2^n n!}} e^{-(y-y_0)^2/2a_B^2} H_n \left( \frac{y-y_0}{a_B} \right), \quad (5.5)$$

where  $a_B = \sqrt{\hbar/m\omega_B}$  and  $H_n$  are the Hermite polynomials. In an area  $\mathcal{A} = L_x L_y$  the number of possible values of  $p_x$  in  $\Delta p_x$  is  $L_x \Delta p_x / 2\pi\hbar$ , where for  $0 < y_0 < L_y$ ,  $\Delta p_x = qBL_y/c$  so that the number of states for given  $n$  and  $p_z$  is  $qBL_x L_y / 2\pi\hbar c = qB\mathcal{A} / 2\pi\hbar c = \Phi/\Phi_0$  where  $\Phi = B\mathcal{A}$  is the magnetic field flux through the area  $\mathcal{A}$  and  $\Phi_0 = hc/q$  is the fundamental magnetic flux quantum.

Landau quantization is a key ingredient in explanation of the *integer quantum Hall effect* [35]. The energy spectrum of the semiconductor in a strong magnetic field forms Landau levels that can be labeled by integer indexes. In addition, the Hall resistivity also exhibits discrete levels labeled by an integer  $\nu$ . The fact that these two quantities are related can be shown in different ways, but most easily can be seen from *Drude model* [36]: the Hall conductivity depends on the electron density  $n$  as  $\sigma_{xy} = 1/\rho_{xy} = ne/B$ . Since the resistivity plateau is given by  $\rho_{xy} = 2\pi\hbar c/e^2\nu$  the required density is  $n = B\nu/\Phi_0$ , which is exactly the density required to fill the Landau level. The gap between different Landau levels along with large degeneracy of each level renders the resistivity quantized.

## B. The Laughlin problem

Laughlin [3] chooses gauge with  $\mathbf{A} = B(x\hat{\mathbf{y}} - y\hat{\mathbf{x}})/2$  so that again  $\mathbf{B} = \hat{\mathbf{z}}B$  and  $\nabla \mathbf{A} = 0$ . Neglecting the electron spin he has

$$H = -\frac{\nabla^2}{2m} - \frac{qB}{2mc} \left( x\frac{\partial}{\partial y} - y\frac{\partial}{\partial x} \right) + \frac{q^2 B^2}{8mc^2} (x^2 + y^2). \quad (5.6)$$

He then finds

$$E_{\mu\nu} = \left( \nu + \frac{1}{2} \right) \hbar\omega_B, \quad (5.7)$$

$$\psi_{\mu\nu} = \frac{1}{\pi^{1/2} a_B^{1/2} \sqrt{2^{\mu+\nu+1} \mu! \nu!}} e^{(x^2+y^2)/4a_B^2} \left( \frac{\partial}{\partial x} + i\frac{\partial}{\partial y} \right)^\mu \left( \frac{\partial}{\partial x} - i\frac{\partial}{\partial y} \right)^\nu e^{-(x^2+y^2)/2a_B^2}, \quad (5.8)$$

for the  $\nu$ th Landau level which is constituted by the manifold of eigenstates with energy  $E_{\mu\nu}$ . The ground state is then

$$\psi_{\mu 0} = \frac{1}{\pi^{1/2} a_B^{1/2} \sqrt{2^{\mu+1} \mu!}} z^\mu e^{-|z|^2/4a_B^2}, \quad (5.9)$$

with  $z = x + iy$ .

Now note that for the  $z$  component of the angular momentum  $L_z = xp_y - yp_x$

$$L_z \psi_{\mu 0} = \hbar\mu \psi_{\mu 0}. \quad (5.10)$$

For  $N$  electrons at  $z_i$  with  $i = 1, 2, \dots, N$  he proposes the following

$$\Psi_{\mu 0} \propto \prod_{j < k} (z_j - z_k)^\mu e^{-\sum_k |z_k|^2/4a_B^2}, \quad (5.11)$$

where  $z_j - z_k$  is the relative coordinate between electron  $j$  and  $k$  and since one wants antisymmetry under exchange of electrons  $\mu$  must be odd. So

$$|\Psi_{\mu 0}|^2 \propto e^{-2\Phi/\mu}, \quad (5.12)$$

$$\Phi = -\sum_{j < k} \mu^2 \ln |z_j - z_k| + \frac{\mu}{4a_B^2} \sum_k |z_k|^2. \quad (5.13)$$

Comparing with Eq. (3.5) we see that this is the potential energy of a two-dimensional one-component plasma where the charges of the particles are equal to  $\mu$  and the background density is  $\mu/2\pi a_B^2$ .

This ansatz, proposed by Robert Laughlin for the variational ground state of a two dimensional electron gas placed in a uniform background magnetic field in the presence of a uniform jellium background when the filling factor of the lowest Landau level is  $\bar{\nu} = 1/\mu$  where  $\mu$  is an odd positive integer. It was constructed to explain the observation of the  $\bar{\nu} = 1/3$  fractional quantum Hall effect [37], and predicted the existence of additional  $\bar{\nu} = 1/\nu$  states as well as quasiparticle excitations with fractional electric charge  $e/\nu$ , both of which were later experimentally observed. Laughlin received one third of the Nobel Prize in Physics in 1998 for this discovery.

In Fig. 2 we compare the experimental results for the integer Hall effect and for the fractional Hall effect.

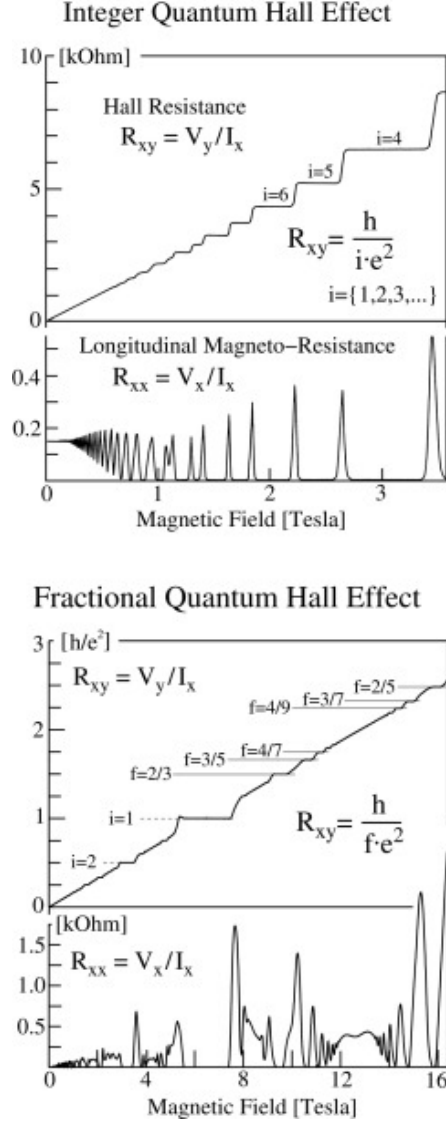


FIG. 2. Quantum Hall effect. On top the integer one and on the bottom the fractional one.

## VI. THE NELSON-KOSTERLITZ PHASE TRANSITION

In Ref. [5] Nelson and Kosterlitz use renormalization method of Ref. [38] to study the behavior of the superfluid density defined in Ref. [39] at the superfluid phase transition.

In a superfluid two-dimensional film of helium atoms of mass  $m$ , in thermal equilibrium at an inverse temperature

$\beta = 1/k_B T$  with  $k_B$  the Boltzmann constant, with a density  $\rho_0$ , we may expand the velocity field as [5]

$$\mathbf{v}_s(\mathbf{q}) = \frac{\hbar}{m} \nabla \varphi(\mathbf{q}) + \left( \frac{2\pi\hbar}{m} \right) (\hat{\mathbf{z}} \times \nabla) \int d\mathbf{q}' n(\mathbf{q}') G(\mathbf{q}, \mathbf{q}'), \quad (6.1)$$

where the first term is a potential flow, with  $\varphi$  a smoothly varying function, and the second is due to the vortices, where  $n$  is an integer valued vorticity field.  $\hat{\mathbf{z}}$  is a unit vector perpendicular to the plane of the film,  $\nabla$  is a gradient, and the Green function  $G(\mathbf{q}, \mathbf{q}')$  satisfies

$$\nabla^2 G(\mathbf{q}, \mathbf{q}') = \delta(\mathbf{q} - \mathbf{q}'), \quad (6.2)$$

$$G(\mathbf{q}, \mathbf{q}') = \frac{1}{2\pi} \left( \ln \frac{|\mathbf{q} - \mathbf{q}'|}{L} + C \right), \quad (6.3)$$

where  $L$  is a constant length,  $C$  is a constant number, and  $\delta$  is the Dirac delta function.

The probability distribution for the superfluid velocity  $\mathbf{v}_s$  is

$$P \propto e^{-H}, \quad (6.4)$$

$$H = \int d\mathbf{q} \left[ \frac{1}{2} \beta \rho_0 v_s^2 + \left( \frac{m}{2\pi\hbar} \right)^2 \ln y_0 (\nabla \times \mathbf{v}_s)^2 \right], \quad (6.5)$$

where the first term is the *kinetic energy* and the second is the *enstrophy* which is peculiar to two dimensional hydrodynamics [40]. The parameter  $\ln y_0$  is the thermodynamically conjugate variable to the enstrophy [38].

Noticing that the gradients are all parallel one another and orthogonal to the  $z$  axis we find

$$v_s^2 = \left( \frac{\hbar}{m} \right)^2 (\nabla \varphi)^2 + \left( \frac{2\pi\hbar}{m} \right)^2 \left[ \nabla \int d\mathbf{q}' n(\mathbf{q}') G(\mathbf{q}, \mathbf{q}') \right]^2, \quad (6.6)$$

and integrating by parts and using Eq. (6.3)

$$\int d\mathbf{q} v_s^2 = \int d\mathbf{q} \left( \frac{\hbar}{m} \right)^2 (\nabla \varphi)^2 - \left( \frac{2\pi\hbar}{m} \right)^2 \left[ \frac{1}{2\pi} \int_{|\mathbf{q}-\mathbf{q}'|>L} \frac{d\mathbf{q}}{L} \frac{d\mathbf{q}'}{L} n(\mathbf{q}) n(\mathbf{q}') \left( \ln \frac{|\mathbf{q}-\mathbf{q}'|}{L} + C \right) \right]. \quad (6.7)$$

Moreover, using again Eq. (6.3),

$$\begin{aligned} \nabla \times \mathbf{v}_s &= \left( \frac{2\pi\hbar}{m} \right) \hat{\mathbf{z}} \nabla^2 \int d\mathbf{q}' n(\mathbf{q}') G(\mathbf{q}, \mathbf{q}') \\ &= \left( \frac{2\pi\hbar}{m} \right) \hat{\mathbf{z}} n(\mathbf{q}). \end{aligned} \quad (6.8)$$

Now putting together Eq. (6.5), (6.7), and (6.8) we find

$$H \approx \frac{1}{2} K \int d\mathbf{q} (\nabla \varphi)^2 - \pi K \int_{|\mathbf{q}-\mathbf{q}'|>L} \frac{d\mathbf{q}}{L} \frac{d\mathbf{q}'}{L} n(\mathbf{q}) n(\mathbf{q}') \ln \frac{|\mathbf{q}-\mathbf{q}'|}{L} + \ln y \int_{|\mathbf{q}-\mathbf{q}'|>L} \frac{d\mathbf{q}}{L} \frac{d\mathbf{q}'}{L} n(\mathbf{q}) n(\mathbf{q}'), \quad (6.9)$$

where  $K = \beta \rho_0 (\hbar/m)^2$  and  $y = y_0 e^{-\pi K C}$  and we approximated  $\int d\mathbf{q} n^2$  with  $(\int d\mathbf{q} n)^2$ .

The superfluid density may be expressed as [39, 41, 42]

$$K_R^{-1} = \frac{m^2}{\hbar^2 \beta \rho_s(T)} = \left( \frac{m}{\hbar} \right)^2 \int d\mathbf{q} \langle \mathbf{v}_s(\mathbf{q}) \mathbf{v}_s(\mathbf{0}) \rangle_P, \quad (6.10)$$

where  $\langle \dots \rangle_P$  is the average respect to the probability distribution  $P$  of Eq. (6.4). Using Gaussian functional integrals we readily see from Eq. (6.9) that

$$\langle n(\mathbf{q}) n(\mathbf{0}) \rangle_P = -2 \frac{1}{2[\pi K \ln(r/L) - \ln y]} \approx -2y^2 (r/L)^{-2\pi K}, \quad (6.11)$$

where we expanded around  $r \sim L$ . So from Eq. (6.7) we find

$$K_R^{-1} = K^{-1} + 16\pi\pi^3 y^2 \int_L^\infty \frac{dr}{L} \left( \frac{r}{L} \right)^{3-2\pi K}. \quad (6.12)$$

For  $3 - 2\pi K > -1$  the integral diverges and the theory breaks down.

### A. Renormalization method

To proceed further we introduce

$$L = L_0 e^{\mathcal{L}} \quad 0 < \mathcal{L} \ll 1, \quad (6.13)$$

and split the integral [38]

$$\int_{L_0}^{\infty} \frac{dr}{L_0} = \int_{L_0}^{L_0 e^{\mathcal{L}}} \frac{dr}{L_0} + \int_{L_0 e^{\mathcal{L}}}^{\infty} \frac{dr}{L_0}. \quad (6.14)$$

The second part gives

$$16\pi^3 y^2 \int_{L_0 e^{\mathcal{L}}}^{\infty} \frac{dr}{L_0} \left( \frac{r}{L_0} \right)^{3-2\pi K} = 16\pi^3 y^2 (e^{\mathcal{L}})^{3-2\pi K} e^{\mathcal{L}} \int_{L_0}^{\infty} \frac{dr}{L_0} \left( \frac{r}{L_0} \right)^{3-2\pi K}, \quad (6.15)$$

where we may define a renormalized  $y$

$$y' = y e^{(2-\pi K)\mathcal{L}} \approx y + (2 - \pi K) \mathcal{L} y, \quad (6.16)$$

so that

$$\frac{y' - y}{\mathcal{L}} \approx \frac{dy}{d\mathcal{L}} = (2 - \pi K)y, \quad (6.17)$$

with  $y(\mathcal{L} = 0) = y$ . On the other hand from the first part of the integral we may renormalize  $K$  as

$$(K^{-1})' = K^{-1} + 16\pi^3 y^2 (e^{\mathcal{L}} - 1) \approx K^{-1} + 16\pi^3 y^2 \mathcal{L}, \quad (6.18)$$

or

$$\frac{(K^{-1})' - K^{-1}}{\mathcal{L}} \approx \frac{dK^{-1}}{d\mathcal{L}} = 16\pi^3 y^2, \quad (6.19)$$

with  $K(\mathcal{L} = 0) = K$ . Then we found that

$$K_R^{-1} = K^{-1}(\mathcal{L}) + 16\pi^3 y^2(\mathcal{L}) \int_L^{\infty} \frac{dr}{L} \left( \frac{r}{L} \right)^{3-2\pi K(\mathcal{L})}. \quad (6.20)$$

can be determined by the ‘‘dressed’’ (renormalized) quantities  $K(\mathcal{L})$  and  $y(\mathcal{L})$ .

Below the critical temperature for the superfluid transition,  $T \leq T_c$ ,

$$\lim_{\mathcal{L} \rightarrow \infty} y(\mathcal{L}) = 0, \quad (6.21)$$

and

$$K_R^{-1} = \lim_{\mathcal{L} \rightarrow \infty} K^{-1}(\mathcal{L}) = \pi/2, \quad (6.22)$$

where in the first equality we used Eq. (6.20) and in the second we used Eq. (6.17). We then found that [5]

$$\lim_{T \rightarrow T_c^-} \frac{m^2}{\hbar^2 \beta \rho_s(T)} = \frac{\pi}{2}, \quad (6.23)$$

a universal constant independent of the initial values of  $K$  and  $y$ .

## VII. CALCULATION OF THE SUPERFLUID FRACTION WITH PATH INTEGRAL

The basis for most *quantum simulations* is *imaginary time path integrals* [43].

Quite generally we will consider a fluid of particles of mass  $m$  in an Euclidean space at  $R = (\{\mathbf{r}_i\}) = (\mathbf{r}_1, \mathbf{r}_2, \dots)$  interacting with the following Hamiltonian

$$H = -\lambda \nabla_R^2 + V(R), \quad (7.1)$$

where we denote with  $\lambda = \hbar^2/2m$  and  $\nabla_R = \sum_i \nabla_{\mathbf{r}_i}$  and  $V$  is the potential energy.

The *density matrix* of the fluid in thermal equilibrium at an inverse temperature  $\beta = 1/k_B T$  with  $k_B$  the Boltzmann constant is

$$\rho(\beta) = e^{-\beta H}, \quad (7.2)$$

and satisfies to the *Bloch equation*

$$\frac{\partial \rho(\beta)}{\partial \beta} = -H \rho(\beta), \quad (7.3)$$

with the boundary condition

$$\rho(0) = \text{Id} \quad (7.4)$$

where  $\text{Id}$  is the identity operator.

### A. Algorithm description

In a Path Integral Monte Carlo (PIMC) simulation of a fluid of  $N$  particles <sup>1</sup> at  $R = (\mathbf{r}_1, \mathbf{r}_2, \dots, \mathbf{r}_N)$  in  $d$  dimensions  $\mathbf{r}_i = (r_{i,1}, r_{i,2}, \dots, r_{i,d})$  in a region of space of measure  $\Omega$  in thermal equilibrium at an inverse temperature  $\beta$ , we measure quantities  $\mathcal{O}$ , diagonal in position representation, through the following averaging

$$\langle \mathcal{O} \rangle = \frac{1}{Z} \sum_{\mathcal{P}} \text{sgn}(\mathcal{P}) \int \rho(R, \mathcal{P}R; \beta) \mathcal{O}(R) dR, \quad (7.5)$$

where the sum is over all  $N!$  permutations of the particles at  $R$  weighted with a sign  $\text{sgn}(\mathcal{P})$ , the integral over  $R$  is multidimensional of dimension  $Nd$ , and <sup>2</sup>

$$\rho(R, R'; \beta) = \langle R | \rho(\beta) | R' \rangle = \int \prod_{k=0}^{M-1} [\rho(R_k, R_{k+1}; \tau) dR_k] \delta(R_0 - R) \delta(R_M - R') dR_M, \quad (7.6)$$

is the position representation of the density matrix where we have discretized the imaginary time  $\beta$  into  $M$  timeslices with a small timestep  $\tau = \beta/M$ , a bead  $R_k = (\{\mathbf{r}_{i,k}\}) = (\{r_{i,j,k}\})$  at each timeslice  $k = 1, 2, \dots, M$ ,  $\delta$  is a  $dN$  dimensional Dirac delta function. We will also call *link* a pair of contiguous beads. Here

$$\rho(R, R'; \tau) = (4\pi\lambda\tau)^{-dN/2} e^{-(R-R')^2/4\lambda\tau} e^{-\tau V(R)}, \quad (7.7)$$

is the high temperature *primitive approximation* for the density matrix, and

$$Z = \sum_{\mathcal{P}} \text{sgn}(\mathcal{P}) \int \rho(R, \mathcal{P}R; \beta) dR, \quad (7.8)$$

is the canonical *partition function*.

The high temperature density matrix of Eq. (7.7) holds for a fluid in a periodic hypercubic simulation box of side  $L$  in flat Euclidean space such that  $L^2 \gg \lambda\tau$  [45]. In Appendix A we will present other expressions valid in the more general case of a Riemannian manifold.

The integral in (7.6) is multidimensional of high dimension  $dNM$ . Then the rule for the measure in (7.5) can be recast into

$$\langle \mathcal{O} \rangle = \oint \Pi \mathcal{O} / \oint \Pi, \quad (7.9)$$

$$\Pi(\{R_k\}, \mathcal{P}) = \text{sgn}(\mathcal{P}) \prod_{k=0}^{M-1} \rho(R_k, R_{k+1}; \tau) \delta(R_0 - R) \delta(R_M - \mathcal{P}R) \quad (7.10)$$

$$= e^{-\mathcal{S}(s)} \text{sgn}(\mathcal{P}) \delta(R_0 - R) \delta(R_M - \mathcal{P}R), \quad (7.11)$$

$$\oint \dots = \sum_{\mathcal{P}} \int dR_0 dR_1 \cdots dR_M \dots, \quad (7.12)$$

<sup>1</sup> We are excluding here anyonic statistics and internal properties of the particles like spin, ....

<sup>2</sup> This convolution product discretized path integral form is possible as long as *Trotter formula* [44] is valid which requires the potential energy to be bounded from below. This is not the case for a Coulomb system where it is necessary to construct the density matrix starting from a pair density matrix as building block.

where  $\mathcal{S}(s) = \mathcal{K}(s) + \mathcal{V}(s)$  is the action and  $s$  is the  $(\{R_k\})$  space. We require  $\pi = \Pi/\oint\Pi$  to be a probability distribution. In other words it must be everywhere positive in the  $(\{R_k\}, \mathcal{P})$  space. We will also need the splitting  $\pi = \pi_0 \tilde{\pi}$  with  $\tilde{\pi} = e^{-\mathcal{V}}/\oint\Pi$  the *inter-action distribution*. The action will then read

$$\mathcal{S}(s) = \sum_{k=0}^{M-1} \left\{ \frac{dN}{2} \ln(4\pi\lambda\tau) + \frac{(R_k - R_{k+1})^2}{4\lambda\tau} + \tau V(R_k) \right\}. \quad (7.13)$$

## B. The superfluid fraction

It is easy to determine when quantum statistics will be important in a fluid. In the absence of interaction, the size of a path is its thermal wavelength, the standard deviation of the position representation of the ideal gas density matrix

$$\Lambda_\beta = \sqrt{2\beta\lambda}, \quad (7.14)$$

When the size of the path equals the interparticle spacing, roughly  $\rho^{-1/d}$  it is at least possible for the paths to link up by exchanging end points. This relations  $\Lambda_\beta = \rho^{-1/d}$  defines the *degeneracy temperature*

$$T_d = \frac{\rho^{2/d}\hbar^2}{mk_B}. \quad (7.15)$$

For temperatures higher than  $T_d$ , quantum statistics (either bosonic or fermionic) are not very important.

In a liquid state,  $T_d$  gives a surprisingly good estimate of the *superfluid transition temperature*  $T_c$ .

Superfluidity is experimentally characterized by the response of a system to movements of its boundaries. The rotating bucket experiment was first discussed by Landau [46] on the basis of his two-fluids hydrodynamic theory of superfluidity. He predicted that superfluid helium would show an abnormal relation between the energy it takes to spin a bucket and its moment of inertia. Suppose one measures the work needed to bring a container filled with helium to a steady rotation rate. A normal fluid in equilibrium will rotate rigidly with the walls. The work done is  $E = I\omega^2/2$ , where  $I$  is the momentum of inertia and  $\omega$  is the angular rotation rate. On the other hand, a superfluid will stay at rest if the walls rotate slowly, so that a smaller energy is needed to spin up the container. The liquid that stays at rest is the superfluid. Experiments by Andronikashvili [47] confirmed this prediction.

The microscopic properties of interacting Bose systems can be calculated by discretized pat integral computations of the density matrix [45, 48]. In these Monte Carlo simulations only the interparticle potential,  $\hbar$ , and the mass  $m$  of the particles are used. We consider a system of  $N$  particles in a volume  $\Omega$  with a density  $\rho = N/\Omega$  in thermal equilibrium at an inverse temperature  $\beta = 1/k_B T$  with  $k_B$  Boltzmann constant.

We do not assume that the bucket has cylindrical symmetry, so there will be some coupling between the walls of the bucket and the liquid helium, allowing the liquid to come to thermal equilibrium with the walls. The effective moment of inertia is defined as the work done for an infinitesimally small rotation rate,

$$I = \frac{dF}{d\omega^2} \Big|_{\omega=0} = \frac{d\langle \mathcal{L}_z \rangle}{d\omega} \Big|_{\omega=0}, \quad (7.16)$$

where  $F$  is the Helmholtz free energy and  $\mathcal{L}_z$  is the  $z$  component of the angular momentum

$$\mathcal{L} = -i\hbar \sum_{i=1}^N \mathbf{r}_i \times \nabla_i, \quad (7.17)$$

where  $\nabla_i = \nabla_{\mathbf{r}_i}$ . On the other hand, the classical moment of inertia is given by

$$I_c = m \left\langle \sum_{i=1}^N (\mathbf{r}_i \times \hat{z})^2 \right\rangle. \quad (7.18)$$

The ration of the two moments is defined as the normal density  $\rho_n$  and what is missing is the superfluid density  $\rho_s = \rho - \rho_n$

$$\frac{\rho_n}{\rho} = \frac{I}{I_c}. \quad (7.19)$$

Thus the superfluid density is the linear response to an imposed rotation, just as the electrical conductivity is the response to an imposed voltage.

We will here describe two Path Integral Monte Carlo (PIMC) estimators that can be used to measure the *superfluid fraction*  $f_s = \rho_s/\rho \in [0, 1]$  during a computer experiment [45].

### Area estimator

Since statistical mechanics does not require the use of an inertial reference frame we can transform to the frame rotating with the bucket to determine the free energy of rotation. The Hamiltonian in the rotating coordinate system is simply given by

$$\mathcal{H}_\omega = \mathcal{H}_0 - \omega \mathcal{L}_z, \quad (7.20)$$

where  $\mathcal{H}_0$  is the Hamiltonian at rest. Here the extra term comes from the relation  $\theta' = \theta - \omega t$  between the new angle  $\theta'$  in the rotating frame and the one  $\theta$  in the laboratory frame.

Now we have to find a path integral expression for the effective moment of inertia defined in Eq. (7.16). The following identity allows us to take the derivative of the density matrix  $e^{-\beta \mathcal{H}_\omega}$  that contains the parameter  $\omega$ . First we break up the exponential into  $M$  pieces  $e^{-\beta \mathcal{H}_\omega} = (e^{-\tau \mathcal{H}_\omega})^M$  with  $\tau = \beta/M$ ,

$$\frac{de^{-\beta \mathcal{H}_\omega}}{d\omega} = \sum_{k=1}^M e^{-(k-1)\beta \mathcal{H}_\omega/M} \frac{de^{-\beta \mathcal{H}_\omega/M}}{d\omega} e^{-(M-k)\beta \mathcal{H}_\omega/M}. \quad (7.21)$$

Now we take the limit  $M \rightarrow \infty$  and  $k\beta/M \rightarrow t$

$$\frac{de^{-\beta \mathcal{H}_\omega}}{d\omega} = \int_0^\beta dt e^{-t \mathcal{H}_\omega} \frac{d(-\mathcal{H}_\omega)}{d\omega} e^{-(\beta-t) \mathcal{H}_\omega} = \int_0^\beta dt e^{-t \mathcal{H}_\omega} \mathcal{L}_z e^{-(\beta-t) \mathcal{H}_\omega}, \quad (7.22)$$

where in the last equality we used Eq. (7.20). So that Eq. (7.16) becomes

$$I = \text{tr} \left( \int_0^\beta dt \mathcal{L}_z e^{-t \mathcal{H}_\omega} \mathcal{L}_z e^{-(\beta-t) \mathcal{H}_\omega} \right) / Z, \quad (7.23)$$

where  $Z = \text{tr}(e^{-\beta \mathcal{H}_\omega})$  is the canonical partition function. Note that in general we should not assume that the system is invariant under rotations around the  $\hat{z}$  axis so that we may not commute the angular momentum operator with the density matrix in the integrand of Eq. (7.23). Nonetheless we may use the cyclic property of the trace to reorder terms in the integrand.

Using Eq. (7.23) into Eq. (7.19) we express the normal fluid density  $\rho_n$  in terms of the matrix elements involving the system at rest. Now we explicitly evaluate this in terms of discrete path integrals by having the angular momentum operate on the action. Since angular momentum commutes with the internal potential energy, that term will not contribute. One can show [48] that an external potential also does not contribute in the continuum  $M \rightarrow \infty$  limit. In evaluating the sum over  $k$  in Eq. (7.21) there is one tricky point. The  $k = 1$  term must be treated separately, since  $\mathcal{L}_z$  operates twice on one link. That term gives rise to the classical response. When  $\mathcal{L}$  acts on the  $k$ th link of the high temperature density matrix  $\rho_k \propto e^{-\sum_i (\mathbf{r}_{i,k} - \mathbf{r}_{i,k+1})^2 / 4\lambda\tau}$  we find  $i\hbar \sum_i [\mathbf{r}_{i,k} \times (\mathbf{r}_{i,k} - \mathbf{r}_{i,k+1})] \rho_k / 2\lambda\tau = -i\hbar (\mathbf{r}_{i,k} \times \mathbf{r}_{i,k+1}) \rho_k / 2\lambda\tau$ , where the  $i$  index runs over the  $N$  particles, the  $k$  index labels the  $M$  timeslices and  $\lambda = \hbar^2 / 2m$ . Noticing that the two angular momentum operators acts on two independent links upon averaging over all the  $M$  links we arrive at the following result

$$f_s = \frac{\rho_s}{\rho} = 1 - \frac{\rho_n}{\rho} = \frac{2m \langle A_z^2 \rangle}{\beta \lambda I_c}, \quad (7.24)$$

$$\mathbf{A} = \frac{1}{2} \sum_{i,k} \mathbf{r}_{i,k} \times \mathbf{r}_{i,k+1}, \quad (7.25)$$

$$I_c = m \left\langle \sum_{i,k} (\mathbf{r}_{i,k} \times \hat{z}) \cdot (\mathbf{r}_{i,k+1} \times \hat{z}) \right\rangle. \quad (7.26)$$

Note that the area (7.25) of a path is a vector. For rotations about the  $z$  axis we need only the  $z$  component of the area. By symmetry the average value of  $\mathbf{A}$  vanishes. Equation (7.24) is the main result of this section and is an exact fluctuation-dissipation formula. The superfluid density is proportional to the mean squared area of paths sampled for a container at rest divided by the classical moment of inertia.

Superfluidity is a microscopic property that can be defined in a finite system. It is not necessary to take the thermodynamic limit or to have a phase transition to see its effect. In the high temperature limit  $f_s \rightarrow 0$  since the paths become short and straight and in the low temperature limit  $f_s \rightarrow 1$  since the paths are long and the thermal average in Eq. (7.23) sums up to zero.

### Winding estimator

Now let us change the geometry of the rotating cylinder, so we can see how superfluidity manifests itself in periodic boundary conditions. Periodic boundary conditions are more convenient for simulations, since no surfaces appear and there is no curvature in making a loop around the boundaries. Instead of using a filled cylinder, we enclose the fluid between two cylinders of mean radius  $R$  and spacing  $d$ , where  $d \ll R$ . The classical moment of inertia will be  $I_c = mNR^2$  and the area (7.25) can be written as  $A_z = WR/2$  where  $W$  is the *winding number*, defined as the flux of paths winding around the torus, times the circumference of the torus. Here we have ignored all nonwinding paths, those paths which do not make a complete circuit around the cylinder, since their contribution is  $\mathcal{O}(R^{-2})$  and negligible at large  $R$ . Now substituting these values of  $A_z$  and  $I_c$ , into Eq. (7.24) for the superfluid density and keeping into account the periodic boundary conditions along the  $d$  space dimensions (a hypertorus is topologically equivalent to the usual periodic boundary conditions), we get<sup>3</sup>

$$\frac{\rho_s}{\rho} = \frac{\langle W^2 \rangle L^2}{2d\lambda\beta N}, \quad (7.27)$$

where the winding number is defined by

$$\mathbf{W} = \frac{1}{L} \sum_{i=1}^N \int_0^\beta dt \left[ \frac{d\mathbf{r}_i(t)}{dt} \right]. \quad (7.28)$$

Usually one applies periodic boundary conditions in all three spatial directions. Then the winding number becomes a vector, just as the area was a vector. But in contrast to the area, it is “quantized” in units of the box length. The winding number is a topological invariant of a given path; one can determine the winding number by counting the flux of paths across any plane; it does not matter where the plane is inserted. We can think of these winding paths as the imaginary time version of circulating currents.

*In d = 2*

It has been predicted theoretically [4, 5] and observed experimentally [49] that for  ${}^4\text{He}$  films the superfluid density jumps from 0 to the universal value of Eq. (6.23)

$$\rho_s(T_c^-) = \frac{m}{\pi} \frac{k_B T_c^-}{\lambda} \quad (7.29)$$

just below the transition. In the present language this says that the average squared winding number,  $\langle W^2 \rangle$ , jumps from 0 to  $2m/\pi$  just below the transition, independent of particle density and periodic cell size.

In Fig. 3 we show the results from a path integral Monte Carlo simulation for a two dimensional  ${}^4\text{He}$  film. The solid line is obtained integrating the Eqs. (6.17) and (6.19) with initial conditions  $K(\mathcal{L} = 0) = \beta\hbar^2\sigma/m^2$ ,  $y(\mathcal{L} = 0) = e^{-\beta E_c}$ , and integration limits from  $\mathcal{L} = 0$  to  $\mathcal{L} = \ln(L/2d)$ , with  $L$  being the size of the simulation cell and the two free parameters,  $E_c$  (“vortex core energy”) and  $d$  (“vortex core radius”) are obtained by a least-squares fit to the simulation results. The dotted line indicates the limit for  $L \rightarrow \infty$ .

## VIII. CONCLUDING REMARKS

We discussed how it is interesting to study the properties of a (quantum) *many body* system at low (non-zero) temperature on a *curved surface*. For example colloidal particles may be adsorbed or confined on a substrate with nonzero curvature, be it the wall of a porous material, or a membrane, a vesicle, a micelle for example made of amphiphilic surfactant molecules such as lipids, or a biological membrane, or the surface of a large solid particle, or an interface in an oil-water emulsion [12]. For a fluid of  ${}^4\text{He}$  atoms it would be interesting to study the superfluid fraction. For a fluid of electrons it would be interesting to study the superfluidity. Moreover it would be interesting to study the properties of the electron plasma on a sphere in presence of a magnetic field.

One important point to discuss is whether the space in which the particles live is exactly two dimensional, as it happens in the satirical novella of Edwin Abbott Abbott [51], or if it can be treated as *quasi* two dimensional.

---

<sup>3</sup> We could have made the whole derivation directly in the periodic space by calculating the response of a periodic system to a linear velocity of its walls. What appears in Eq. (7.23) in place of  $\mathcal{L}$  is the total linear momentum operator [48].

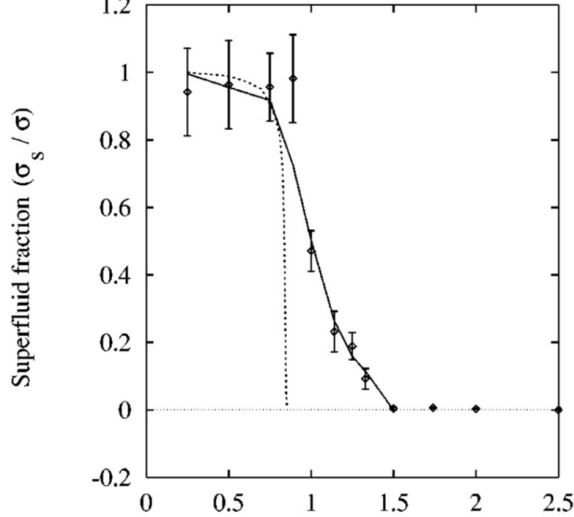


FIG. 3. Superfluid fraction versus temperature for a two dimensional  $^4\text{He}$  film with a coverage  $\sigma = 0.0508\text{\AA}^{-2}$ . The diamonds are the simulation results, while the solid line is the result of a least-squares fitting procedure. The dotted line is the result of the application of the Nelson-Kosterlitz theory to a system with the same parameters, in the limit of infinite area. Result from Ref. [50].

There is a profound difference between the two scenarios to the point that the form of the interaction between the particles also changes. For example for colloidal particles one may choose the polarizable hard sphere pair interaction or for the fluid of helium atoms one may use the Lennard Jones pair potential, but the distance between the two interacting particles may be chosen either as the geodesic distance between them or the Euclidean distance in the three dimensional space where the surface is embedded. For the electron gas the Coulomb pair potential as a solution to the Poisson equation has different forms in two or three dimensions and in general depends on the metric of the curved surface.

These properties can be studied exactly with the (path integral) Monte Carlo method and these studies certainly enrich the knowledge on many bodies in (quantum) general relativity [52–56]. Not even the two body problem can be treated analytically in general relativity [57]. The problem of gravitating many bodies should be separated by the problem of many bodies with non-gravitational interactions in general relativity. In fact mass curves spacetime through the Einstein field equations and gravitating bodies will behave as free particles on that curved spacetime, whereas non-gravitational interactions produce particles accelerations on the spacetime. So being able to treat many (quantum) bodies on a curved surface would be an important step forward for the much more complicated problem of gravitating many (quantum) bodies in general relativity.

We find it of fundamental importance issuing a bridge between the two scientific communities of the exact simulations of a many body (quantum) system and of general relativity. We foresee an important progress in the physics of (quantum) gravitating many body systems beyond the simple ideal gases or hydrodynamic systems that are usually treated [6, 32].

#### Appendix A: The high temperature density matrix on Riemannian manifolds

On a Riemannian manifold of dimension  $d$  and metric tensor  $g_{\mu\nu}(\mathbf{r})$ , the geodesic distance between two infinitesimally close points  $R$  and  $R'$  is  $d\tilde{s}^2(R, R') = \sum_{i=1}^N ds^2(\mathbf{r}_i, \mathbf{r}'_i)$  where  $ds^2(\mathbf{r}, \mathbf{r}') = g_{\mu\nu}(\mathbf{r} - \mathbf{r}')^\mu(\mathbf{r} - \mathbf{r}')^\nu$ . Moreover,

$$\tilde{g}_{\mu\nu}(R) = g_{\alpha_1\beta_1}(\mathbf{r}_1) \otimes \dots \otimes g_{\alpha_N\beta_N}(\mathbf{r}_N), \quad (\text{A1})$$

$$\tilde{g}(R) = \prod_{i=1}^N \det \|g_{\alpha_i\beta_i}(\mathbf{r}_i)\|, \quad (\text{A2})$$

where  $\|\tilde{g}_{\mu\nu}\|$  is a matrix made of  $N$  diagonal blocks  $\|g_{\alpha_i\beta_i}\|$  with  $i = 1, 2, \dots, N$ . The Laplace-Beltrami operator on the manifold of dimension  $dN$  is

$$\Delta_R = \tilde{g}^{-1/2} \nabla_\mu (\tilde{g}^{1/2} \tilde{g}^{\mu\nu} \nabla_\nu), \quad (\text{A3})$$

where  $\nabla = \nabla_R$ ,  $\tilde{g}^{\gamma\nu}$  is the inverse of  $\tilde{g}_{\gamma\nu}$ , i.e.  $\tilde{g}_{\mu\gamma}\tilde{g}^{\gamma\nu} = \delta_\mu^\nu$  the Kronecker delta, and a sum over repeated indexes is tacitly assumed.

We will assume that  $\mathcal{H}$  in curved space has the same form (7.1) as in flat space <sup>4</sup>

$$\mathcal{H} = -\lambda \Delta_R + V(R). \quad (\text{A4})$$

In the small  $\tau$  limit Eq. (7.7) now becomes

$$\rho(R, R'; \tau) \propto \tilde{g}(R)^{-1/4} \sqrt{D(R, R'; \tau)} \tilde{g}(R')^{-1/4} e^{\lambda\tau\mathcal{R}(R)/6} e^{-\mathcal{S}(R, R'; \tau)}, \quad (\text{A5})$$

where  $\mathcal{R}$  is the scalar curvature of the curved manifold <sup>5</sup>,  $\mathcal{S}$  the action, and  $D$  the van Vleck's determinant [59, 60]

$$D_{\mu\nu} = \nabla_\mu \nabla'_\nu \mathcal{S}(R, R'; \tau), \quad (\text{A6})$$

$$\det \|D_{\mu\nu}\| = D(R, R'; \tau), \quad (\text{A7})$$

where  $\nabla = \nabla_R$  and  $\nabla' = \nabla_{R'}$ . For this propagator the volume element for integration is  $\sqrt{\tilde{g}(R)} dR$ . In the expression (A5) the two factors  $\tilde{g}^{-1/4}$  are needed in order to have for the density matrix a bidensity for which the boundary condition to Bloch equation is simply a Dirac delta function  $\rho(R, R'; 0) = \delta(R - R')$ . The square root of the van Vleck determinant factor takes into account the density of paths among the minimum extremal region for the action (see Chapter 12 of Ref. [60]).

For the action and the kinetic-action we have <sup>6</sup>

$$\mathcal{S}(R, R'; \tau) = \mathcal{H}(R, R'; \tau) + \tau V(R), \quad (\text{A8})$$

$$\mathcal{H}(R, R'; \tau) = \frac{dN}{2} \ln(4\pi\lambda\tau) + \frac{d\tilde{s}^2(R, R')}{4\lambda\tau}. \quad (\text{A9})$$

In particular the kinetic-action is responsible for a diffusion of the random walk with a variance of  $2\lambda\tau/\tilde{g}_{\mu\nu}$ .

### On a sphere

A sphere of radius  $a$  is the surface,  $d = 2$  <sup>7</sup>, of constant positive scalar curvature  $2/a^2$  so that  $\mathcal{R} = 2N/a^2$  and in the small  $\tau \rightarrow 0$  limit  $\tilde{g}(R)^{-1/4} \sqrt{D(R, R'; \tau)} \tilde{g}(R')^{-1/4} \rightarrow (1/2\lambda\tau)^N$ . So we see how both the curvature and the van Vleck factors, being constant, simply drop off from the measure of the various observables of Eq. (7.5). Yet from a calculation of one free quantum particle on the sphere we will face the *hairy ball theorem*, according to which the Euler class is the obstruction to the tangent plane of the sphere having a nowhere vanishing section, i.e. fiber or hair. The theorem was first proven by Henri Poincaré for the sphere in 1885 [61], and extended to higher even dimensions in 1912 by Luitzen Egbertus Jan Brouwer [62]. The theorem has been expressed colloquially as “you can't comb a hairy ball flat without creating a cowlick” or “you can't comb the hair on a coconut” as shown in Fig. 4. If  $z$  is a continuous function that assigns a vector in the three dimensional space to every point  $\mathcal{P}$  on a sphere such that  $z(\mathcal{P})$  is always tangent to the sphere at  $\mathcal{P}$ , then there is at least one pole, a point where the field vanishes, i.e. a  $\mathcal{P}$  such that  $z(\mathcal{P}) = 0$ . Every zero of a vector field has a (non-zero) index <sup>8</sup>, and it can be shown that the sum of all of the indexes at all of the zeros must be two, because the Euler characteristic of the sphere is two. Therefore, there must be at least one zero. This is a consequence of the *Poincaré-Hopf theorem*. The theorem was proven for two dimensions by Henri Poincaré and later generalized to higher dimensions by Heinz Hopf [63]. In particular we see how, even a single free particle have a path which will be subject to some anisotropy due to the effective potential induced by the curvature of the sphere. This effect was studied in Refs. [64, 65].

We plan in the near future to determine the superfluid fraction for a fluid of <sup>4</sup>He atoms on a sphere using the area estimator (7.24). We also plan to use affine quantization [52, 56] to fix the ordering ambiguities in Eq. (A4).

<sup>4</sup> This is a delicate point and should be studied more carefully [52]. Especially for what concerns ordering ambiguities. We here appeal to simplicity.

<sup>5</sup> The factor depending on the curvature of the manifold is due to Bryce DeWitt [58]. For a space of constant curvature there is clearly no effect, as the term due to the curvature just leads to a constant multiplicative factor that has no influence on the measure of the various observables. One might have hoped that certain constrained coordinates, perhaps a relative coordinate in a molecule, would effectively live in a space of variable curvature. Perhaps gravitation will give us the system on which the effect of curvature can be seen, but at present the effect is purely in the realm of theory.

<sup>6</sup> The expression for  $\mathcal{H}$  is the one of Eq. (24.16) of Ref. [60] at lowest order.

<sup>7</sup> So it is conformally flat.

<sup>8</sup> The index of a bilinear function/al is the dimension of the space on which it is negative definite. According to Morse theorem, from the calculus of variations, there is a relation between the conjugate points (a point of the path where the path cease to be a minimum of the action) along a classical path to the negative eigenvalues of  $\delta^2 S$ . More precisely Morse index theorem states that, for an extremum  $R(t)$ ,  $0 < t < \beta$  of  $S$ , the index of  $\delta^2 S$  is equal to the number of conjugate points to  $R(0)$  along the path  $R(t)$  (each such conjugate point is counted with its multiplicity). In the context of vector fields on a Riemannian manifold the index is equal to +1 around a source or a sink, and more generally equal to  $(-1)^k$  around a saddle that has  $k$  contracting dimensions and  $n - k$  expanding dimensions.

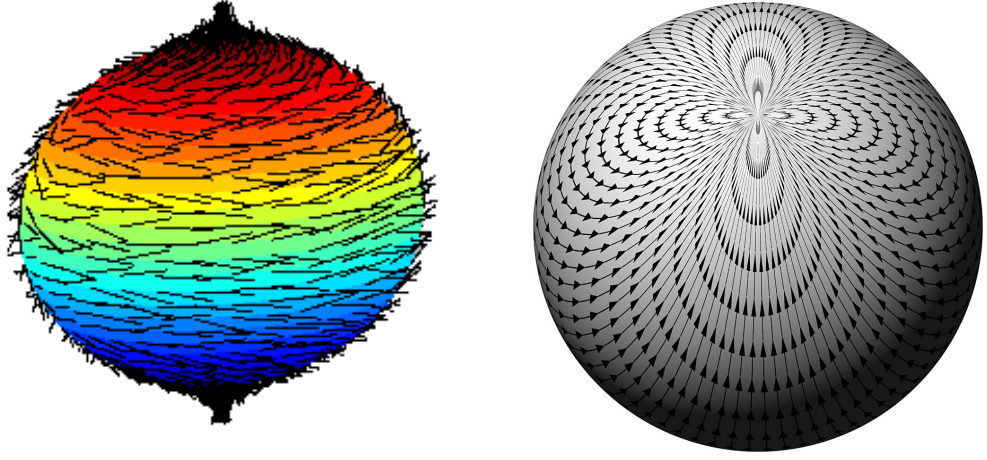


FIG. 4. On the left, pictorial view of a hairy ball; on the right, a continuous tangent vector field on a sphere with only one pole, in this case a dipole field with index 2. A path of a quantum particle on the sphere will be “combed”.

## AUTHOR DECLARATIONS

### Conflicts of interest

None declared.

### Data availability

The data that support the findings of this study are available from the corresponding author upon reasonable request.

### Funding

None declared.

- [1] N. H. March and M. P. Tosi, *Coulomb Liquids* (Academic Press Inc Ltd, London, 1984).
- [2] R. Fantoni, Plasma living in a curved surface at some special temperature, *Physica A* **177**, 524 (2019).
- [3] R. B. Laughlin, Anomalous quantum Hall effect: An incompressible quantum fluid with fractionally charged excitations, *Phys. Rev. Lett.* **50**, 1395 (1983).
- [4] J. M. Kosterlitz and D. J. Thouless, Ordering, metastability and phase transitions in two-dimensional systems, *J. Phys. C: Solid State Phys.* **6**, 1181 (1973).
- [5] D. R. Nelson and J. M. Kosterlitz, Universal Jump in the Superfluid Density of Two-Dimensional Superfluids, *Phys. Rev. Lett.* **39**, 1201 (1977).
- [6] C. W. Misner, K. S. Thorne, and J. A. Wheeler, *Gravitation* (W. H. Freeman, San Francisco, 1973).
- [7] P. A. Martin, Sum rules in charged fluids, *Rev. Mod. Phys.* **60**, 1075 (1988).
- [8] B. Jancovici, Exact Results for the Two-Dimensional One-Component Plasma, *Phys. Rev. Lett.* **46**, 386 (1981).
- [9] A. Alastuey and B. Jancovici, On the classical two-dimensional one-component Coulomb plasma, *J. Phys. (France)* **42**, 1 (1981).
- [10] P. Debye and E. Hückel, Zur theorie der elektrolyte, *Phys. Z.* **9**, 185 (1923).
- [11] J. M. Caillol, D. Levesque, J. J. Weis, and J. P. Hansen, A monte carlo study of the classical two-dimensional one-component plasma, *J. Stat. Phys.* **28**, 325 (1982).

- [12] R. Fantoni, J. W. O. Salari, and B. Klumperman, The structure of colloidosomes with tunable particle density: Simulation vs experiment, *Phys. Rev. E* **85**, 061404 (2012).
- [13] S. F. Edwards and A. Lenard, Exact Statistical Mechanics of a One Dimensional System with Coulomb Forces. II. The Method of Functional Integration, *J. Math. Phys.* **3**, 778 (1961).
- [14] R. Fantoni, Exact results for one dimensional fluids through functional integration, *J. Stat. Phys.* **163**, 1247 (2016), erratum DOI 10.1007/s10955-016-1519-7.
- [15] J. Ginibre, Statistical Ensembles of Complex, Quaternion, and Real Matrices, *J. Math. Phys.* **6**, 440 (1965).
- [16] M. L. Metha, *Random Matrices* (Academic, New York, 1967).
- [17] M. L. Rosinberg and L. Blum, The ideally polarizable interface: A solvable model and general sum rules, *J. Chem. Phys.* **81**, 3700 (1984).
- [18] B. Jancovici, G. Manificat, and C. Pisani, Coulomb systems seen as critical systems: Finite-size effects in two dimensions, *J. Stat. Phys.* **76**, 307 (1994).
- [19] B. Jancovici and G. Téllez, Coulomb systems seen as critical systems: Ideal conductor boundaries, *J. Stat. Phys.* **82**, 609 (1996).
- [20] P. Choquard, *Helv. Phys. Acta* **54**, 332 (1981).
- [21] P. Choquard, P. J. Forrester, and E. R. Smith, The two-dimensional one-component plasma at  $\Gamma = 2$ : The semiperiodic strip, *J. Stat. Phys.* **33**, 13 (1983).
- [22] J. M. Caillol, Exact results for a two-dimensional one-component plasma on a sphere, *J. Phys. (France) - Lett.* **42**, L (1981).
- [23] G. Téllez and P. J. Forrester, Exact Finite-Size Study of the 2D OCP at  $\Gamma = 4$  and  $\Gamma = 6$ , *J. Stat. Phys.* **97**, 489 (1999).
- [24] B. Jancovici, Pressure and Maxwell Tensor in a Coulomb Fluid, *J. Stat. Phys.* **99**, 1281 (2000).
- [25] R. P. Salazar and G. Téllez, Exact Energy Computation of the One Component Plasma on a Sphere for Even Values of the Coupling Parameter, *J. Stat. Phys.* **164**, 969 (2016).
- [26] B. Jancovici and G. Téllez, Two-Dimensional Coulomb Systems on a Surface of Constant Negative Curvature, *J. Stat. Phys.* **91**, 953 (1998).
- [27] R. Fantoni, B. Jancovici, and G. Téllez, Pressures for a One-Component Plasma on a Pseudosphere, *J. Stat. Phys.* **112**, 27 (2003).
- [28] B. Jancovici and G. Téllez, Charge Fluctuations for a Coulomb Fluid in a Disk on a Pseudosphere, *J. Stat. Phys.* **116**, 205 (2004).
- [29] R. Fantoni and G. Téllez, Two dimensional one-component plasma on a Flamm's paraboloid, *J. Stat. Phys.* **133**, 449 (2008).
- [30] A. K. Geim and K. S. Novoselov, The rise of graphene, *Nature Materials* **6**, 183 (2007).
- [31] R. Fantoni, The density of a fluid on a curved surface, *J. Stat. Mech.* , P10024 (2012).
- [32] S. L. Shapiro and S. A. Teukolsky, *Black Holes, White Dwarfs, and Neutron Stars. The Physics of Compact Objects* (John Wiley & Sons Inc, New York, 1983).
- [33] L. D. Landau and E. M. Lifshitz, *Quantum mechanics*, Course of Theoretical Physics, Vol. 3 (Butterworth Heinemann, 1977) translated from the Russian by J. B. Sykes and M. J. Kearsley, edited by E. M. Lifshitz and L. P. Pitaevskii. Section §111, 112.
- [34] L. D. Landau, Diamagnetismus der Metalle, *Zeitschrift für Physik* **64**, 629 (1930).
- [35] E. Hall, On a New Action of the Magnet on Electric Currents, *American Journal of Mathematics* **2**, 287 (1879).
- [36] P. Drude, Zur Elektronentheorie der Metalle, *Annalen der Physik* **306**, 566 (1900).
- [37] D. C. Tsui, H. L. Stormer, and A. C. Gossard, Two-Dimensional Magnetotransport in the Extreme Quantum Limit, *Phys. Rev. Lett.* **48**, 1559 (1982).
- [38] J. U. José, L. P. Kadanoff, S. Kirkpatrick, and D. R. Nelson, Renormalization, vortices, and symmetry-breaking perturbations in the two-dimensional planar model, *Phys. Rev. B* **16**, 1217 (1977).
- [39] R. P. Feynman, Application of Quantum Mechanics to Liquid Helium, *Prog. Low Temp. Phys.* **1**, 17 (1955).
- [40] R. H. Kraichnan, Statistical dynamics of two-dimensional flow, *•* **67**, 155 (1975).
- [41] L. Onsager, Statistical hydrodynamics, *Nuovo Cimento Suppl.* **6**, 279 (1949).
- [42] P. C. Hohenberg and P. C. Martin, Microscopic theory of superfluid helium, *Ann. Phys.* **34**, 291 (1965).
- [43] R. P. Feynman, The  $\lambda$ -Transition in Liquid Helium, *Phys. Rev.* **90**, 116 (1953).
- [44] H. F. Trotter, On the Product of Semi-Groups of Operators, *Proc. Am. Math. Soc.* **10**, 545 (1959).
- [45] D. M. Ceperley, Path integrals in the theory of condensed Helium, *Rev. Mod. Phys.* **67**, 279 (1995).
- [46] L. D. Landau, The theory of superfluidity of helium II, *J. Phys. USSR* **5**, 71 (1941).
- [47] E. L. Andronikashvili, A direct observation of two kinds of motion in helium II, *J. Phys. USSR* **10**, 201 (1946).
- [48] E. L. Pollock and D. M. Ceperley, Path-integral computation of superfluid densities, *Phys. Rev. B* **36**, 8343 (1987).
- [49] J. Bishop and J. D. Reppy, Study of the Superfluid Transition in Two-Dimensional  $^4\text{He}$  Films, *Phys. Rev. Lett.* **40**, 1727 (1978).
- [50] M. C. Gordillo and D. M. Ceperley, Path-integral calculation of the two-dimensional  $^4\text{He}$  phase diagram, *Phys. Rev. B* **58**, 6447 (1998).
- [51] E. A. Abbott, *Flatland: A Romance of Many Dimensions* (Seeley & Co., London, 1884).
- [52] J. R. Klauder and R. Fantoni, The Magnificent Realm of Affine Quantization: valid results for particles, fields, and gravity, *Axioms* **12**, 911 (2023).
- [53] R. Fantoni, Statistical Gravity through Affine Quantization, *Quantum Rep.* **6**, 706 (2024).
- [54] R. Fantoni, Statistical Gravity and entropy of spacetime, *Stats* **8**, 23 (2025).

- [55] R. Fantoni, Statistical Gravity, ADM splitting, and Affine Quantization, *Gravitation and Cosmology* **31** (2025).
- [56] R. Fantoni, *Unifying Classical and Quantum Physics - How classical and quantum physics can pass smoothly back and forth* (Springer, New York, 2025).
- [57] R. Fantoni, Relaxation in scalar gravitational field theory, *Gravitation and Cosmology* **32**, 2026 (2025).
- [58] B. S. DeWitt, Dynamical Theory in Curved Spaces. I. A Review of the Classical and Quantum Action Principles, *Rev. Mod. Phys.* **29**, 377 (1957).
- [59] J. H. V. Vleck, The Correspondence Principle in the Statistical Interpretation of Quantum Mechanics, *Proc Natl Acad Sci U S A* **14**, 178 (1928).
- [60] L. S. Schulman, *Techniques and Applications of Path Integration* (John Wiley & Sons, Technion, Haifa, Israel, 1981) chapter 24.
- [61] H. Poincaré, Sur les courbes définies par les équations différentielles, *Journal de Mathématiques Pures et Appliquées* **4**, 167 (1885).
- [62] L. E. J. Brouwer, Über Abbildung von Mannigfaltigkeiten, *Mathematische Annalen* **71**, 97 (1912).
- [63] H. Hopf, Vektorfelder in n-dimensionalen Mannigfaltigkeiten, *Math. Ann.* **96**, 209 (1926).
- [64] R. Fantoni, One-component fermion plasma on a sphere at finite temperature, *Int. J. Mod. Phys. C* **29**, 1850064 (2018).
- [65] R. Fantoni, One-component fermion plasma on a sphere at finite temperature. The anisotropy in the paths conformations, *J. Stat. Mech.* , 083103 (2023).